Analyst

PAPER

View Article Online
View Journal | View Issue

Cite this: *Analyst*, 2019, **144**, 611

Cerebrospinal fluid levels of alpha-synuclein measured using a poly-glutamic acid-modified gold nanoparticle-doped disposable neuro-biosensor system†

Münteha Nur Sonuç Karaboğa *[a] and Mustafa Kemal Sezgintürk[b]

Alpha-synuclein (SYN) is a prominent key protein in Parkinson-type dementia. Measurement of the amount of this protein found in the cerebrospinal fluid (CSF) using precise techniques may help in the diagnosis and prognosis of the disease. In this study, a gold nanoparticle (AuNP)–polyglutamic acid (PGA)-modified indium tin oxide (ITO)-based disposable neuro-biosensor system was designed for alpha-synuclein (alpha-SYN), an important biomarker of Parkinson's disease. Glutamic acid was formed by electropolymerization on the electrode surface. The parameters that can affect the performance of the biosensing probe were optimized. The techniques used in the design of the immobilization steps, the optimization studies, and the evaluation of the analytical performance of the targeted neuro-biosensor are electrochemical impedance spectroscopy (EIS), cyclic voltammetry (CV) and square wave voltammetry (SWV). Charge transfer resistance (R_{ct}) changes were highly linear and sensitive with the alpha-SYN concentration in the 4–2000 pg mL^{-1} range and associated with a limit of detection of 0.135 pg mL^{-1}. With the designed disposable neuro-biosensor system, the amount of alpha-SYN found in CSF samples was determined by the standard addition technique and found to be strikingly sensitive to the target analyte. Morphological and chemical changes on the sensing surface were evaluated by scanning electron microscopy (SEM) and Fourier transform infrared spectroscopy (FTIR). In addition, it was determined that the PGA-modified, AuNP-doped neuro-biosensor system has great reproducibility potency, long storage stability, and regeneration capacity. We suggest that the AuNP–PGA combination platform is ideal for use as a biosensing probe to detect alpha-SYN.

Received 12th July 2018,
Accepted 23rd October 2018

DOI: 10.1039/c8an01279b

rsc.li/analyst

Introduction

Parkinson's disease (PD) represents the most common movement disorder and the second most common neurodegenerative disease of the central nervous system.[1] Intraneuronal protein aggregates composed largely of α-synuclein are found in all Parkinson's patients.[2,3] Recent research has shown that α-synuclein monomers can acquire neurotoxic properties by first following a pathogenic process of oligomers, followed by small protofibrils and finally large and insoluble α-synuclein fibrils.[4–6]

PD can be diagnosed after clinical manifestations occur, and when diagnosed, the median or late level of the disease is reached.[7] However, neurodegeneration owing to the disease begins years before diagnosis.[8] Furthermore, apart from limited clinical and brain imaging assessment, there is no objective and/or effective method to monitor the progression of typically expensive Parkinson's disease or assess the efficacy of experimental treatments.[9] Early diagnosis of Parkinson's disease is prioritized in light of current efforts to improve the treatment of the disease. In addition, increasing the diagnostic sensitivity of Parkinson's disease will also allow it to separate from other types of dementia that are very similar to it.[10,11]

The synuclein family comprises soluble small proteins in alpha, beta and gamma forms. Alpha-SYN, a relatively small protein of 140 amino acids, is extensively expressed in presynaptic terminals in the brain. Alpha-SYN constitutes 1% of the total soluble protein in cytosolic brain fractions, suggesting that it may play an important role in neuronal function. Although α-SYN is essentially an intracellular protein, it is also present in biological fluids such as cerebrospinal fluid (CSF), blood and plasma.[12,13]

Recent studies have emphasized that alpha-synuclein may be an important biomarker in Parkinson's disease. It is

[a]*Namik Kemal University, School of Health, Tekirdag, Turkey.*
E-mail: mnsonuc@nku.edu.tr
[b]*Canakkale Onsekiz Mart University, Faculty of Engineering, Bioengineering, Canakkale, Turkey*

†Electronic supplementary information (ESI) available. See DOI: 10.1039/c8an01279b

assumed that higher levels of the soluble oligomeric form of alpha-synuclein may indicate a pathogenic species in Parkinson's disease. It has been shown that soluble α-synuclein oligomers break down membranes in both *in vitro* and animal models and subsequently cause cell death.[9,12–16] In addition to serum, a promising alternative approach for clinical examination is the use of biochemical markers in CSF. Monitoring changes in the alpha-synuclein in the CSF is of particular importance in diagnosing the disease,[14,17] since biochemical processes affecting neuropathological changes or critical functional pathways in the brain directly affect the composition of the CSF.[18]

Neuroimaging techniques used in the diagnosis of PD provide very valuable information, but they help in diagnosis after the clinical symptoms have occurred. However, the specificity of some of these tools are low; the half-life of labeled elements used in some of them are short and the techniques are relatively expensive. All of these situations limit the usability of neuroimaging techniques.[19,20]

Neuro-biosensors and disposable sensors have advantages such as (i) rapid display of the clinical status, (ii) determination of disease progression, (iii) determination of resistance to the patient's weakness/disease, and (iv) self-evaluation by a patient. In addition, neurodegenerative disease sensors may be a complementary element in disease management by monitoring diet, exercise, and drug effects.[21] Even when a CSF sample is required for the detection of analytes of neurodegenerative diseases, the process can be faster and more precise than conventional tests.[22,23]

From this point, we developed a disposable neuro-biosensor system for the efficient and sensitive determination of alpha-SYN, a potent candidate biomarker for Parkinson's disease. The design of the neuro-biosensor, optimization of parameters and analytical performances were studied by electrochemical impedance spectroscopy (EIS), cyclic voltammetry (CV) and square wave voltammetry (SWV). The morphological and chemical changes on the surface were evaluated by scanning electron microscopy (SEM), Fourier transform infrared spectroscopy (FTIR) and SEM-energy dispersive X-ray (EDX) mapping. The validation of the designed neuro-biosensor in clinical practice was performed by analyzing target analytes in CSF.

Among the various semiconductor electrodes, indium-tin oxide (ITO) electrodes are promising for the characterization of biological systems. ITO surfaces maintain their stability under physiological conditions due to their polarizable properties. In addition, PET-coated ITO substrates were used as a working electrode throughout this study because of their high electrical conductivity, low capacitive current, electrochemical activity over a wide potential range, and stable physical and electrochemical properties.[24,25]

Materials and methods

Reagents and apparatus

Reference (Ag/AgCl), counter (platinum wire) and working electrodes (disposable ITO-coated PET films, 2 × 0.5 cm) were supplied from BASi (West Lafayette, IN, USA) and Sigma Aldrich (St Louis, MO, USA). Alpha-synuclein from human plasma (product no S7820) and monoclonal anti-synuclein antibody from mouse were obtained from Sigma Aldrich (St Louis, MO, USA). SYN and anti-SYN stock solutions prepared with pH 7.0 phosphate buffer at certain concentrations were maintained at −20 °C until used. Gold(III) chloride trihydrate and glutamic acid were supplied from Sigma Aldrich (St Louis, MO, USA).

5 mM $[Fe(CN)_6]^{4-}$ and 5 mM $[Fe(CN)_6]^{3-}$ containing 1 M KCl were prepared in 50 mM phosphate buffer using it as a redox probe. The CSF samples were obtained with research ethics committee approval numbered 2013/86/07/05 from Namık Kemal University, Faculty of Medicine.

The morphological changes that occurred in each design step of the neurobiosensor were studied by Scanning Electron Microscopy (SEM, FEI-Quanta FEG 250). Measurements of changes in chemical bonds were performed by Attenuated Total Reflection Fourier Transform Infrared (ATR-FTIR) using a Bruker Company Vertex 70 FTIR infrared spectrometer (4000–400 cm^{-1}).

Preparation of disposable electrodes and deposition of gold nanoparticles

The first step in preparing the neuro-biosensor is to clean the ITO-PET disposable electrode surface. For this purpose, the ITO electrodes were sonicated for 10 minutes in acetone, soap solution and ultrapure water, respectively, and then dried with ultrapure argon gas. In order to make further modifications to the surface of the cleaned ITO electrodes, it is necessary to form active-hydroxyl groups on the surface. The hydroxyl groups on the surface are formed by the technique previously reported.[26] Afterwards, electrodes washed with ultrapure water and dried with argon gas were immersed in an electrochemical cell containing $HAuCl_4{\cdot}3H_2O$ (1 mM) solution prepared in 50 mM pH 7.0 phosphate buffer. The electrochemical deposition of gold nanoparticles on the ITO surface was carried out with 10 cycles at a scan rate and potential from −0.2 V to −1.3 V at 50 mV s^{-1}.[27] Then, the gold nanoparticle-doped electrodes were washed with ultrapure water, dried with argon gas and stored in a dark environment.

Design strategy of the alpha-SYN neuro-biosensor

ITO electrodes with gold nanoparticles deposited on the surface were modified by the electropolymerization of the glutamic acid monomer. For this purpose, the electrodes were immersed in the glutamic acid solution prepared in 50 mM pH 7.0 phosphate buffer and electropolymerization was carried out at a potential range of −0.8 V to +2.0 V (100 mV s^{-1}, 10 cycles).[28] The electrodes were incubated for 60 min at room temperature by immersing in an aqueous solution containing 0.4 mM EDC and 0.1 mM NHS for the activation of the carboxylic acid terminal groups of polyglutamic acid (PGA) and covalent interactions of these groups with the amino groups in the anti-alpha-SYN antibody. Electrodes washed with ultra-pure water and dried with ultra-pure argon gas were then

immersed in 100 μL anti-alpha-SYN-containing solutions and allowed to incubate for 60 minutes at room temperature in the dark. After incubation with the anti-alpha-SYN antibody, the electrodes were washed with ultrapure water to remove unbound antibody molecules and then dried with argon gas. Finally, gold nanoparticle-doped poly-glutamic acid-modified electrodes immobilized with anti-alpha-SYN were incubated for 60 minutes in a 0.5% BSA solution to block non-reactive ends and prevent non-specific interactions. With this last step, the prepared neurobiosensor was maintained at +4 °C until alpha-SYN measurements were performed. Clean and modified ITO surfaces were expressed as ITO, ITO–OH, ITO–OH–AuNP, ITO/AuNP/PGA, ITO/AuNP/PGA/anti-alpha-SYN and ITO/AuNP/PGA/anti-alpha-SYN/BSA. The design strategy of the biosensor is schematized in Scheme 1.

Electrochemical measurements

The evaluation of the immobilization steps, the optimization tests and the analytical performance of the developed system was carried out on the basis of the parameters of our previous studies with EIS (initial frequency: 50 000 Hz, final frequency: 0.05 Hz, points: 5, formal potential: 0 V), CV (potential between −500 mV and 1000 mV, scan rate: 100 mV s^{-1}, step size: 10 mV) and SWV (potential scan range: 0–1.2 V, and pulse size: 25 mV).[29]

Measurement principle of alpha-SYN

Each gold nanoparticle-doped, glutamic acid-modified disposable ITO-based electrode was incubated with standard alpha-SYN solutions prepared at different concentrations for 60 minutes at room temperature and in the dark. After incubation, the modified neuro-biosensor was gently washed with ultrapure water to clean possible physical adsorbents on the surface. The changes on each disposable surface depending on the changing alpha-SYN concentrations were measured by EIS and CV and the results were recorded with the EChem Analyst software program.

CSF sample analysis

To assess the feasibility and analytical reliability of the developed neurobiosensor, the amount of alpha-SYN in human CSF was analyzed using the standard addition method. The alpha-SYN concentrations used for standard addition are 25 pg mL^{-1} and 500 pg mL^{-1}. CSF samples were collected randomly from the patients and controls. All experiments were performed in accordance with the Guidelines of the Republic of Turkey, Ministry of Health, and approved by the ethics committee at Namik Kemal university. Informed consents were obtained from human participants of this study. CSF samples were maintained at −20 °C in specific portions until measurements were performed.

Results and discussion

Confirmation of the neuro-biosensor fabrication steps by EIS and CV

The gold nanoparticle and the polyglutamic acid polymer were utilized in the neurobiosensor system developed for the determination of alpha-synuclein (alpha-SYN), a Parkinson's disease biomarker. After cleaning the ITO-PET electrodes with

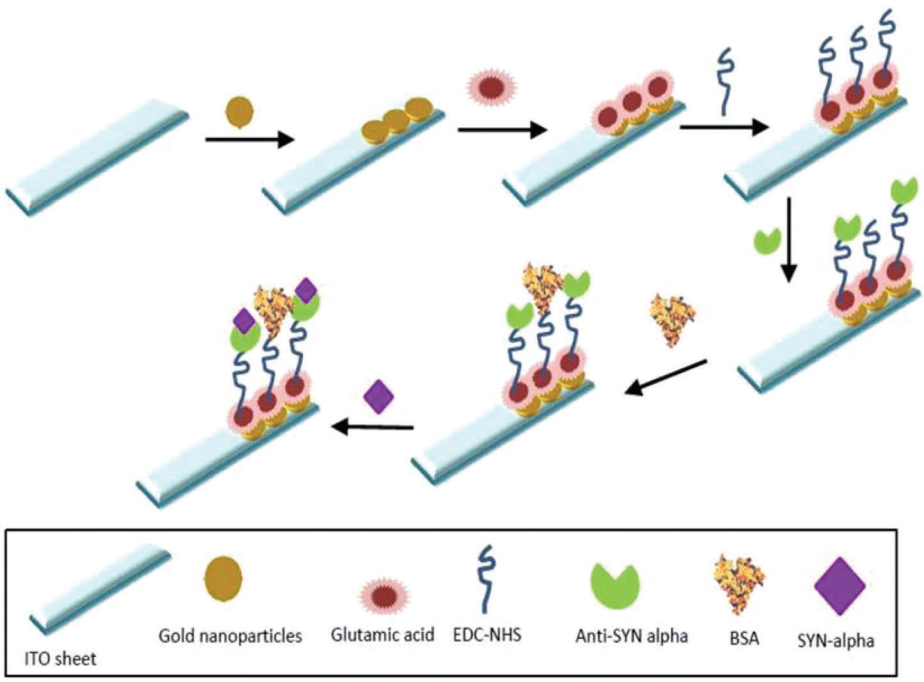

Scheme 1 Schematic illustrations of immobilization steps of anti-alpha-SYN.

the specified technique, active –OH groups were formed on the clean electrode surface. Then, gold nanoparticles were deposited by the electrochemical technique on the surface of the hydroxylated ITO electrodes. The electrochemical approach is a good alternative for producing AuNPs directly on a substrate in a single-step, useful way. With this method, it is relatively easy to control the particle morphology and distribution of AuNPs by altering the deposition potential, concentration, buffer solution and accumulation time. In addition, electrochemical nanoparticle deposition is cheaper, faster and easier to apply than other techniques.[30] Fig. 1 clearly shows the cyclic voltammograms recorded during the electrochemical synthesis of Au nanoparticles by electrochemical deposition. The crossover of the forward and reverse cycles (Fig. 1A) in the first voltammogram emphasizes the importance of surface conditions. When the surface of the electrode is not well cleaned, this crossover is not observed systematically.[31] The reduction of Au at about −940 mV *versus* the Ag/AgCl reference was then shifted to −1.010 V (Fig. 1B) due to the nucleation on accumulation, with a potential for reduction along with recurrent screening cycles. This shift is an indication that the gold nanoparticles have accumulated on the surface. Another point to note is that the $AuCl_4$-cathodic peak current is reduced. This variation is mainly due to $AuCl_4$ consumption in the diffusion layer. When the previous studies were examined, the application of positive potentials of gold nanoparticle deposition on the ITO surface more than −0.2 to −0.4 V prevents successful gold nanoparticle formation. This can be explained by the fact that the applied potential is not sufficient for nucleation but may be sufficient for particle growth. Fig. 1C shows the clean ITO electrode before and after gold nanoparticle deposition.

The cyclic voltammograms in Fig. 2 show the growth of an electrochemically active coating of polyglutamic acid. In the first cycle in the potential range of −0.8 to 2.0 V, glutamic acid exhibited a sharp peak around 1.20 V in connection with the free radical formed.

In the second cycle, the sharp peak disappeared and was replaced by a new point around 1050 volts. This new peak

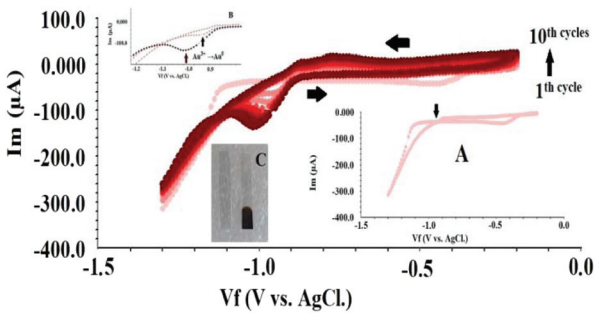

Fig. 1 Cyclic voltammograms of the gold nanoparticle coating on the ITO electrode surface. (A) First cycle, (B) shifted reduction potential of gold nanoparticle generation and (C) bare ITO and gold nanoparticle coated ITO.

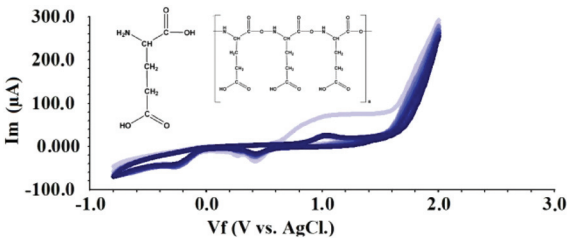

Fig. 2 Cyclic voltammograms of the electro-polymerization of glutamic acid on the gold nanoparticle doped ITO electrode surface.

belongs to the peak of the increased polymer with the number of cycles. Electro-polymerization is observed when the oxidation potential of free radicals is more than 1.5 V, which is more positive. This is the polymerization process initiated by free radical formation. When the anodic potential was increased, it was seen that the electro-polymerization accelerated and the background current increased. Similarly, reducing the cathodic potential up to −0.8 V may increase the reaction. Thus, the electrochemical potential range was applied from −0.8 to 2.0 V. After the ninth cycle, the increase in the peak current is almost constant and more stable; this suggests that the growth of polymerization has reached the level of saturation. Polyglutamic acid is condensed through interactions between a group of carboxylate groups on the glutamic acid and the amino group. This structure liberates carboxylate residues on the AuNP-ITO film surface.

The steps for constructing the developed neuro-biosensor for the alpha-SYN assay are shown in Fig. 3, with the impedance spectra obtained from the EIS, the charge transfer changes for each step, and the voltammograms taken from the CV.

In EIS, the R_{ct} is a manifestation of two effects: (1) electrostatic repulsion with the energy barrier of the redox species reaching the electrode at an energy potential (*i.e.*, excess capacity) related to the reduction and oxidation processes at the bioelectrode or (2) a steric obstacle.[32]

As can be seen from Fig. 3A and B, the gold nanoparticle appears to impart clear conductivity to the bare ITO electrodes. Electrode conducting behavior is still observed when the glutamic acid polymer is formed on the gold nanoparticle-doped surface. The amino groups of anti-alpha-SYN, which covalently interacts with the carboxylate groups of the glutamic acid polymer, cause a barrier on the surface, resulting in increased impedance. The blocking effect of BSA is characterized by an increase in the impedimetric signal as expected.

When the peak potential difference between anodic and cathodic waves (Fig. 3C) was calculated ($\Delta E_p = E_{pc} - E_{pa}$), the ΔE_p value decreased to 0.36 V after the gold nanoparticle was deposited while the ΔE_p value of the hydroxylated ITO electrode was 0.45 V at a scan rate of 100 mV s^{-1}. The peak potential separation, which is inversely proportional to the electron transfer rate, is used for the electrochemical evaluation of the conductivity of the electrode.[33] This decrease shows that electrochemically deposited AuNPs on the ITO surface greatly

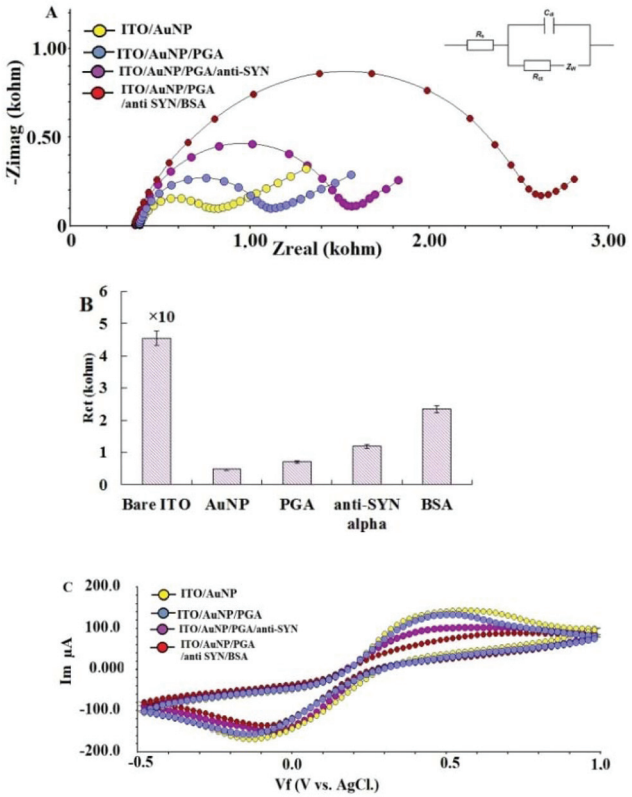

Fig. 3 EIS spectrum (A), charge transfer changes (B) and cyclic voltammograms (C) of immobilization steps.

increase the conductivity of the electrode. After coating the ITO electrodes modified with gold nanoparticles with the polyglutamic acid polymer, the peak current separation decreased to 0.31 V. ΔE_p values indicate that AuNP and PGA provide conductive bridges to increase Fe $(CN)_6^{3-/4-}$ electron transfer and to accelerate the entire oxidation–reduction process.

Optimization studies of the alpha-SYN biosensor

Effect of the monomer concentration. The effectiveness of the electro-polymerization step was increased by optimizing the concentration of the glutamic acid monomer. For this purpose, the response of the neuro-biosensor system, prepared with different monomer concentrations, to the SYN concentrations within a certain range was followed using calibration curves obtained from the EIS data. As shown in ESI Fig. 1,† the charge transfer resistance was gradually increased until reaching a monomer concentration of 50 mM. However, when the glutamic acid concentration reaches 50 mM, the charge transfer kinetics are seriously reduced, which is attributable to the PGA thick film, which inhibits surface contact with the redox probe. However, the 20 mM glutamic acid concentration is optimized for further studies due to the high charge transfer with a relatively high detection coefficient (R^2: 0.9555).

Effect of electro-polymerization cycles. The density of the polyglutamic acid polymer on the gold nanoparticle-doped ITO electrode surface is affected by the number of polymerization cycles. This effect plays a critical role in determining the limit of detection for alpha-SYN by altering the morphology of the surface.

Fig. 2 (ESI†) shows that as the number of cycles increases, the electron transfer resistance increases due to the formation of a thicker PGA film on the surface, and when the number of cycles reaches 20, it is considered that the thickened PGA film inhibits the electron transfer process. While the number of cycles of 20 slows down the sensing process, the number of cycles of 10 has a relatively high detection coefficient (R^2: 0.9557).

Optimum anti-alpha-SYN concentration. At the end of the optimization studies, the effect of the anti-alpha-SYN concentration on the gold nanoparticle–poly glutamic acid-modified biosensing system response was investigated. For this aim, the anti-SYN solutions prepared at different concentrations (11 ng mL^{-1}, 110 ng mL^{-1} and 500 ng mL^{-1}) were immobilized on the sensing surface for 60 min at room temperature. The biosensing system has relatively low charge transfer resistance and detection coefficient (R^2: 0.9555) at the low anti-alpha-SYN concentration (11 ng mL^{-1}). However, because of the high steric hindrance produced by 500 ng mL^{-1} of anti-alpha-SYN, it appears to be rapidly saturated with low concentrations of alpha-SYN. The neuro-biosensor system prepared with the 110 ng mL^{-1} anti-alpha-SYN solution has a high detection coefficient (R^2: 0.9866) (Fig. 3†).

Analytical characteristics of the alpha-SYN neuro-biosensor. Alpha-SYN measurements at different concentrations were performed with the gold nanoparticle-doped PGA-modified disposable neuro-biosensor system, prepared under optimal conditions (Fig. 4A–C).

The relationship between the alpha-SYN concentration and electron transfer resistance is determined by the equivalent circuit model added to Fig. 1A. R_s and Z_W from the elements in the equivalent circuit model represent the diffusion properties of the redox probe in solution and the mass properties of the electrolyte solution. Two components in the model, C_{dl} and R_{ct}, depend on the dielectric and insulation properties at the electrode/electrolyte interface.

The calibration graph of the SYN neuro-biosensor was drawn using the following equation:

$$\Delta R_{ct} = R_{ct}(\mathrm{SYN}) - R_{ct}(\mathrm{BSA})$$

The redox probe provides a faradaic current at the electrode surface when the appropriate potential is applied to the electrode. The changes in the real component of the impedance spectrum observed on the formation of the bio-affinity complex on the electrode surface are higher than the corresponding capacitance variations. The faradaic current due to the increasing standard concentrations of alpha-SYN indicates the presence of an immunocomplex on the surface (Fig. 4A). As the concentration of alpha-SYN increases in the resulting bio-affinity complex, the charge transfer resistance exhibits a linear increase up to a certain point. The curve drawn from the EIS spectrum (Fig. 4B) shows that the developed neuro-biosensor system gives a linear correlation at 4–2000 pg mL^{-1}.

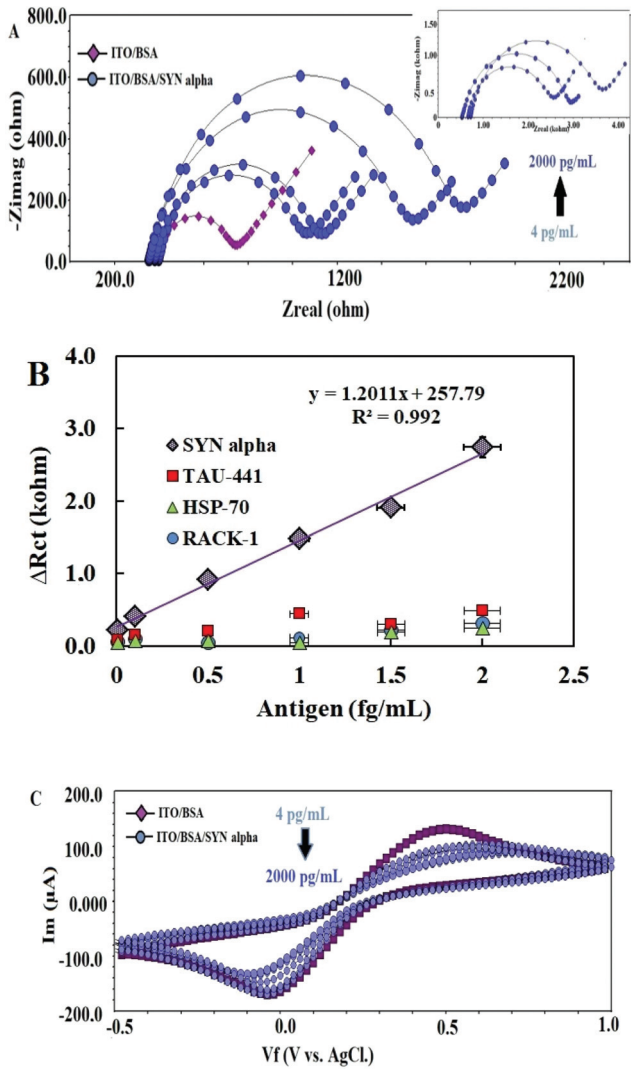

Fig. 4 Impedance spectra obtained for different concentrations of alpha-SYN (A), concentration-dependent calibration curve for alpha-SYN obtained using the biosensor based on anti-SYN under optimal working conditions (B), and cyclic voltammograms (C) obtained for different concentrations of alpha-SYN.

The LOD (limit of detection) and LOQ (limit of quantification) values for alpha-SYN were determined to be 0.135 pg mL^{-1} and 0.45 pg mL^{-1}, respectively, for the gold nanoparticle-doped, polyglutamic acid-modified disposable neuro-biosensor system.

These results emphasize that the developed biosensor shows high sensitivity in alpha-SYN analysis.

The bio-affinity interaction between alpha-SYN and the AuNP–PGA functionalized bioelectrode increases the thickness of the charged bilayer and inhibits the interface electrochemical process of the redox probe. As the electrode capacitance decreases, the electron transfer resistance increases (Table 1). This is the result of the impedimetric behavior of the developed neuro-biosensor system in the range of 4–2000 pg mL^{-1} alpha-SYN.

Table 1 Depending on the increased alpha-SYN concentration, the charge transfer resistance, Ru and capacitance changes

Electrodes	R_{ct} (ohm)	Ru (ohm)	C_{dl} (μF)
Neuro-biosensor	395.8 ± 5.6	399.7 ± 2.90	3.71 ± 0.14
Alpha-SYN 4 pg mL^{-1}	677.3 ± 7.7	407.9 ± 2.91	3.27 ± 0.09
Alpha-SYN 25 pg mL^{-1}	756.8 ± 8.0	392.2 ± 2.86	2.58 ± 0.06
Alpha-SYN 100 pg mL^{-1}	1152 ± 10.9	367.1 ± 2.67	2.49 ± 0.04
Alpha-SYN 500 pg mL^{-1}	1376 ± 12.7	369.4 ± 2.65	2.39 ± 0.04
Alpha-SYN 1000 pg mL^{-1}	1918 ± 18.9	677.2 ± 4.67	2.36 ± 0.05
Alpha-SYN 1500 pg mL^{-1}	2877 ± 26.7	747.2 ± 5.13	2.05 ± 0.04
Alpha-SYN 2000 pg mL^{-1}	3724 ± 25.3	548.3 ± 3.73	2.03 ± 0.03

Kramers Kronig transforms (K.K.T.) are used to calculate the linear, stable and causal circuit spectrum of the developed biosensor. K.K.T. shows a graph of relative errors for the real and imaginary parts of the data of the biosensor design steps. Calculations were made by following the Boukamp method.[34] K.K.T can be shown in the Bode and Nyquist graphs, and if the experimental data do not match K.K.T, interpretation is made under the influence of non-linear, unstable or unknown variables.[35] Table 2 indicates that the K.K. transforms of the AuNP–PGA-based alpha-synuclein biosensor show minimal systematic error and that the used model matches real and imaginary impedance data.

The repeatability of the ITO-based gold nanoparticle and the PGA-doped neuro-biosensor was determined by the analysis of the same concentration of alpha-SYN (100 pg mL^{-1}) with 20 disposable electrodes prepared under similar conditions. The correlation coefficient, the average value, and the standard deviation of the biosensor were calculated as 4.43%, 128.65 pg mL^{-1} and, 5.69 pg mL^{-1}, respectively; so it can be emphasized that the biosensor system has a very good repeatability capacity.

The reproducibility of the AuNP-doped, PGA modified ITO-based alpha-SYN neuro-biosensor was specified by monitoring the responses to the 4–2000 pg mL^{-1} alpha-SYN assay range of six biosensor systems prepared at different times with the same procedure under optimum conditions. Reproducibility studies showed that 6 neuro-biosensor responses showed similar linearity between 4 and 2000 pg mL^{-1} for alpha-SYN. The relative standard deviations of reproducibility slopes and intercepts were found to be 4.54, and 4.0%, respectively. Reproducible signals provide a high reliability and robustness

Table 2 Kramers Kronig transform values of immobilization steps of the neuro-biosensor

Neuro-biosensor steps	Kramers Kronig transform values (μ)
Bare ITO	179.8
ITO/OH	50.02
ITO/OH/AuNP	6.488
ITO/OH/AuNP/PGA	10.177
ITO/OH/AuNP/PGA/anti-SYN	5.688
ITO/OH/AuNP/PGA/anti-SYN/BSA	1.645

assessment of the outcome of the neuro-biosensor response. The immobilization of anti-alpha-SYN on the ITO surface consisting of glutamic acid and the gold nanoparticle platform was achieved with strong covalent interactions. This is fundamental to the fact that the neuro-biosensor has high reproducibility characteristics.

The regeneration capacity of the developed neuro-biosensor was tested by treatment with a pH 2.8 glycine-HCl buffer regeneration solution. The change in pH affects the enthalpy of the system by changing the relative loads between the analyte (alpha-SYN) and the bioreceptor (anti-SYN). As side groups ionize, charge distributions that preserve the tertiary structure of the bioreceptor also change. This denaturation helps to separate the analyte from the bioreceptor.[36] ITO-PET electrodes decorated with gold nanoparticle–polyglutamic acid were able to be regenerated six times with the indicated buffer system. From the 7th cycle, the alpha-SYN signal is lost at a critical level (ESI, Fig. 4†). This can be explained by the complete deterioration of the AuNP–PGA biosensing platform. The biosensing system exhibits high regeneration capacity, offering potential for commercial use by reducing costs.

The sensitivity of the developed neurobiosensor system was also monitored by square wave voltammetry (SWV), an important voltammetric technique. The alpha-SYN standard solutions prepared in the assay range (4–2000 pg mL^{-1}) were measured with a gold nanoparticle–polyglutamic acid decorated neurobiosensor system and a calibration graph was obtained from the resulting voltammograms (Fig. 5).

The results obtained from SWV are similar to the results obtained from the EIS. To compare the two methods, the creation of a calibration graph with the EIS requires the implementation of impedimetric tests in a frequency range, which means a period of serious analysis and effort. In contrast, SWV is a faster detection technique because voltammetric scanning is completed within seconds. As shown, a peak-shaped current response is produced and can be used to directly generate the calibration graph. When a probe with an electrochemically reversible reaction is used in combination with an unlabeled electrochemical biosensor, SWV can be preferred as a rapid, efficient and cost-effective detection technique. As the use of electroactive species is relatively reduced, the ITO electrode surface is less hindered by non-electroactive products. Another advantage of SWV is that due to the reduction of the oxygen present in the background current, it is not necessary to remove the oxygen from the analyte solution.[37]

The selectivity of the designed biosensor for the target alpha-SYN antigen was determined by examining the nonspecific interactions of some nonspecific protein antigens with human HSP-70, Tau-441 and RACK-1 in the same concentration range (4–2000 pg mL^{-1}). The negligible contribution of nonspecific interactions to total R_{ct} response (Fig. 4B) suggests that the biosensor has good selectivity against the specific target alpha-SYN. Selectivity is particularly important in real samples where the target analyte concentration is much less than the concentration of the non-target biomolecules.

Storage stability is the ability of the neurobiosensor system to protect its activity and sense the target analyte when stored under specified conditions after production. This parameter is very important for the commercialization of the biosensor system. Fig. 5 (ESI†) shows the response of the biosensor system to the analyte when stored at +4 °C. It was observed that the sensing system completely retained its activity for 6 weeks and lost 20% of its activity from the 7th week. At the end of the 10th week, the biosensor signal decreased by 60%.

Single frequency impedance (SFI) experiments. Single frequency impedance is used to follow the electrochemical impedance changes of the antibody–antigen interactions in time. Unlike the standard EIS, there is no spectrum for SFI. The measurement is made with a constant DC potential applied to the electrochemical cell. The fixed frequency to be applied to the system was determined with the assistance of the Bode plot (Fig. 6A). The Bode graph shows absolute $Z(\omega)$ and phase

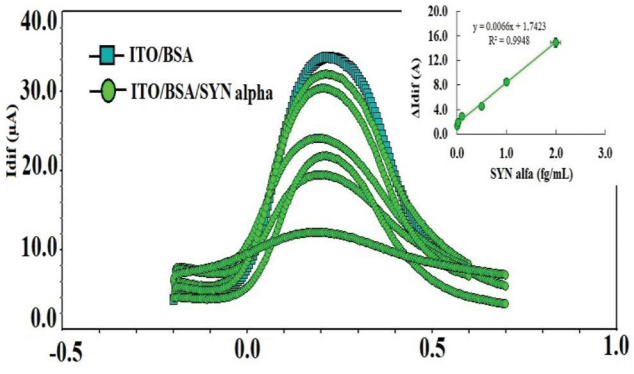

Fig. 5 The response of the neurobiosensor system to different alpha-SYN concentrations by SWV and the calibration graph obtained from SWV.

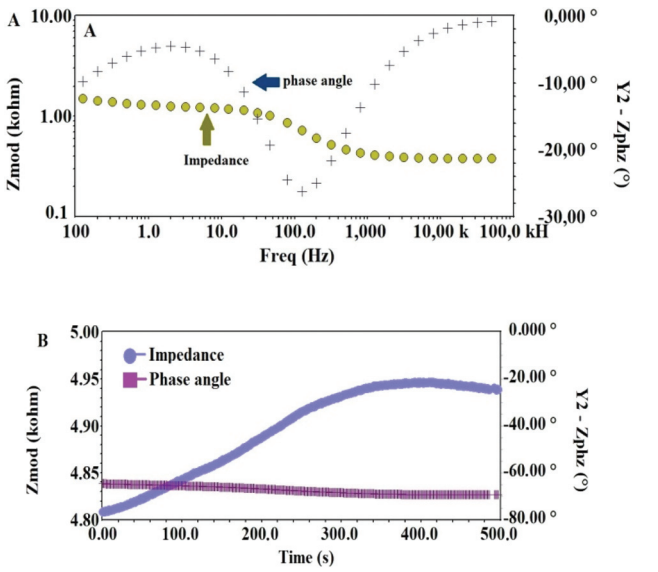

Fig. 6 Bode plot (A) and SFI spectra of the neuro-biosensor.

$\theta(\omega)$ angles within the frequency domain. Since the frequency appears at one of the axes, the effect of the spectrum on the impedance and the phase shift is obvious. The impedimetric behavior of the biosensor system at the fixed frequency (7 Hz) for alpha-SYN determination in a non-faradaic environment is shown in Fig. 6B.

It was observed that at around 550 seconds alpha-SYN is saturated at the biosensing surface. At the impedance, the phase angle shows the strength of the capacitive character. Decreasing the capacitance of the system manifests itself as a decrease in the phase angle. In the faradaic EIS, a redox species is alternately oxidized–reduced. For this reason, the redox-active species and DC conditions must be added to the faradaic EIS environment in such a way that they cannot be consumed. In contrast, no additional reagent is needed for non-faradaic impedance spectroscopy, making non-faradaic studies more suitable for point of care applications. From this point, the analysis of samples with SFI is promising for clinical applications.

Clinical sample applications of the developed neuro-biosensor system. Clinical validation of the developed neuro-biosensor was performed by alpha-SYN analysis in CSF samples collected randomly from healthy individuals and patients with Parkinson's disease who applied to the neurology clinic of Namık Kemal University. The detection of disease-related changes in the brain is the main goal of CSF protein analysis. The increased concentration of the CSF total protein was accepted as a marker of neurological disease shortly after the onset of lumbar burst.[38] Literature reports indicate that the alpha-SYN concentration is at the pg mL^{-1} level in healthy individuals; however, its concentration is increased to ng mL^{-1} in patients with Parkinson's disease.[16,39] The clinical details of the individuals who donated the CSF are given in ESI Table 1.†

In order to evaluate the feasibility and analytical reliability of the neuro-biosensor, different alpha-SYN concentrations (25 pg mL^{-1} and 500 pg mL^{-1}) were added to CSF samples and EIS analysis was performed. Relative standard deviation (RSD) and analytical values of recovery were calculated with the help of a calibration graph. The determination of the concentration of the alpha-SYN biomarker will be informative about the early diagnosis, prognosis and even the mechanism of the disease. When Table 3 is interpreted, we find that the gold nanoparticle-doped polyglutamic acid-modified ITO disposable neurobiosensor system is able to detect the amount of alpha-SYN in the CSF of both healthy individuals and PD patients with high sensitivity. The capacity of the developed neurobiosensor system to identify alpha-SYN, a key protein in the diagnosis and prognosis of PD, is promising in terms of feasibility.

FTIR and SEM studies. The morphological changes on the neuro-biosensor surface were monitored step by step with a scanning electron microscope. Fig. 7A is an SEM image of a bare ITO electrode. After the electrodes are coated with gold nanoparticles, the surface morphology is as shown in Fig. 7B. It is seen that the average size of the AuNP is around 80–100 nm. Nanometer-sized gold particles are known to exhibit excellent catalytic activity due to their large surface-to-volume ratios and the presence of active areas on the surface. After polyglutamic acid polymerization, the morphology of the surface changed again.

The immobilization of anti-alpha-SYN on the AuNP–PGA modified surface is clearly visible in the globular form it acquires as shown in Fig. 7D. While the blocking step with BSA causes morphological changes (Fig. 7E), the globular form of the protein in the last step (Fig. 7F), which is immunocomplexed with the alpha-SYN antibody, is clearly displayed.

The energy-dispersive X-ray spectroscopy (EDX) spectrum of the gold nanoparticle deposition step on the ITO surface is shown in Fig. 6S.† When the SEM images are evaluated together with the spectrum, it can be interpreted that the AuNP is successfully deposited on the electrode surface.

The FTIR spectra of the steps for the formation of polyglutamic acid (a) and the immobilization of anti-alpha-SYN (b) on the neurobiosensor are shown in Fig. 8. The strong peak at about 1720 cm^{-1}, and the vibration at 1250 cm^{-1} shown in

Table 3 Determination of alpha-SYN concentrations in CSF samples with the developed neurobiosensor system

	CSF number	Content of alpha-SYN in the CSF (pg mL^{-1})	The addition content (pg mL^{-1})	The detection content (pg mL^{-1}, $n = 3$)	RSD (%, $n = 3$)	Recovery (%)
Healthy individuals	1	942	25	999.17/990.70/943.22	3.084	101.1
			500	1457.7/1425/1415.9	1.534	99.4
	2	497.9	25	515.5/533.1 /500.5	3.161	98.7
			500	1000.3 /992 /1021	1.486	100.6
	3	403.5	25	415.5 /422.3/417.7	0.816	104
			500	915/918.1/909.4	0.51	102
	4	102	25	137.2/145/148.2	3.967	116
			500	590/585.5/584	0.566	99.6
Patients with Parkinson's disease	1	2555	25	2540.5/2512.3/2440	2.075	96.81
			500	3222/3119/3005.5	3.475	101.98
	2	3947.7	25	3950.5/3922 /3888.8	0.787	98.68
			500	4623.8 /4502 /4871.7	4.037	104.9
	3	3726	25	3666.6 /3730.5/3741	1.084	98.98
			500	4410/4333.8/4179	2.732	101.93
	4	3993.5	25	4010.5/4000.7/3954.2	0.754	99.26
			500	4663/4557.7/4605.5	1.144	102.56

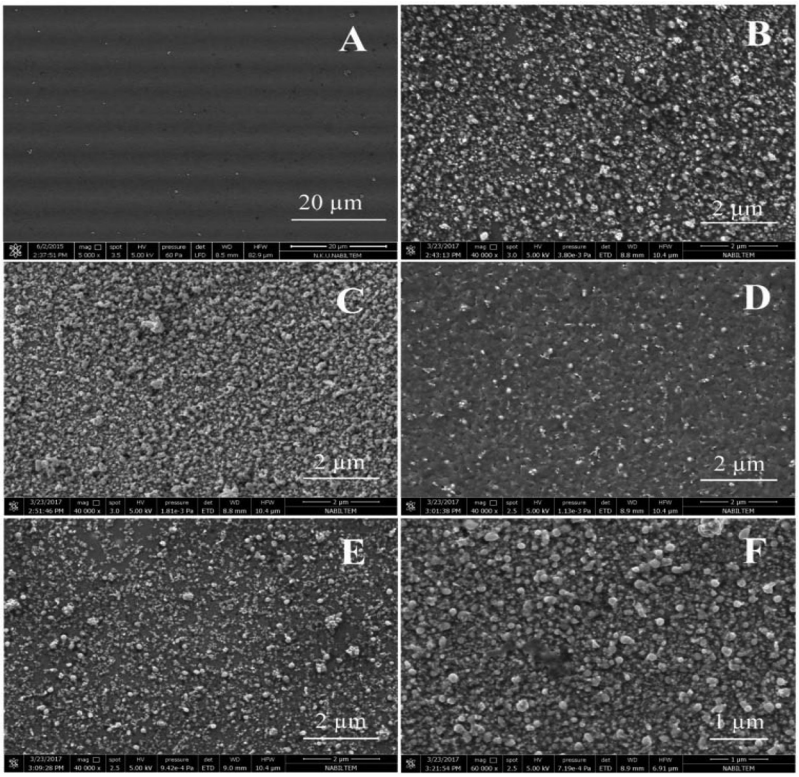

Fig. 7 SEM images related to the morphological changes of the biosensor surfaces: (A) ITO, (B) ITO/AuNP, (C) ITO/AuNP/PGA, (D) ITO/AuNP/PGA/anti-alpha-SYN, (E) ITO/AuNP/PGA/anti-alpha-SYN/BSA, and (F) ITO/AuNP/PGA/anti-alpha-SYN/BSA/ alpha-SYN.

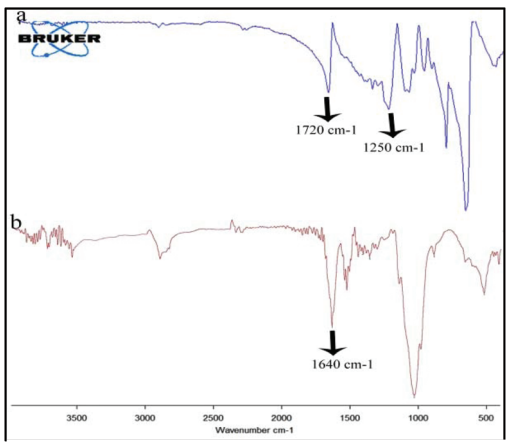

Fig. 8 FTIR spectra of the alpha-SYN neurobiosensor: (a) PGA and (b) anti-alpha-SYN.

Fig. 8A belong to the C–O bond, which indicates the presence of the carboxylate group in the PGA. The peak at 1640 cm^{-1} (Fig. 8B) indicates the covalent bond resulting from the covalent interaction between anti-alpha-SYN and PGA for the formation of the amide bond after anti-alpha-SYN immobilization on the PGA surface.

Although alpha-SYN is an important biomarker for Parkinson-type dementia, a limited number of biosensor studies have been reported in the literature to determine this biomarker. A common feature of these studies is the use of amplification materials to broaden the detection range and reduce the detection limit (Table 4). The AuNP–PGA-added surface platform used in this study increased the sensitivity for alpha-SYN. The neuro-biosensor system developed is different from other studies in this respect. In addition, the practicality of the method and its low cost are key points of the

Table 4 Comparison of the analytical properties of various alpha-SYN biosensors reported in the literature

Electrode configuration	Immobilization procedure	Measurement method	Determination range	LOD	Ref.
Au doped TiO_2 nanotube	Ab_1 interaction	Photo-electrochemical	50 pg mL^{-1}–100 ng mL^{-1}	34 pg mL^{-1}	40
PAMAM–Au nanoparticle carbon electrode	Poli-*o*-ABA covalent interaction	EIS and CV	20 pg mL^{-1}–200 ng mL^{-1}	14.6 pg mL^{-1}	41
Thiolated aptamer gold electrode	Aggregation of AuNPs	EIS, SPR	0.1 nM–0.5 μM	1.0 pg mL^{-1}	42
AuNP–PGA doped ITO electrode	EDC-NHS chemistry	EIS ve CV	4–2000 pg mL^{-1}	0.135 pg mL^{-1}	Present

study. Alpha-SYN is also present in the serum but the body fluid that is critical to the diagnosis is CSF. The designed neuro-biosensor system is distinct from the studies presented in the literature by analyzing alpha-SYN in CSF samples with high sensitivity at the pg mL^{-1} level.

Conclusion

Studies have shown that the expression of the alpha-SYN biomarker increases in the early stages of Parkinson's disease. The gold nanoparticle-doped and polyglutamic acid-modified biosensing platform allowed alpha-SYN to be detected in a range of 4–2000 pg mL^{-1}. It emphasizes that the developed neuro-biosensing system has a wide detection range at the level of the picogram and is a bio-sensing probe that can detect even the smallest change in the protein concentration.

ITO-PET, used as a working electrode, is a disposable and useful material which is open to modification. In addition, long storage stability, poor affinity to different proteins, reproducible results, and high sensitivity for the relevant analyte in the CSF are important points in the present study.

Conflicts of interest

There are no conflicts to declare.

References

1 J. Parkinson, *J. Neuropsychiatry Clin. Neurosci.*, 2002, **14**, 223–236.
2 K. Vekrellis, M. Xilouri, E. Emmanouilidou, H. J. Rideout and L. Stefanis, *Lancet Neurol.*, 2011, **10**, 1015–1025.
3 M. A. Nalls, N. Pankratz, C. M. Lill, C. B. Do, D. G. Hernandez, M. Saad, A. L. DeStefano, E. Kara, J. Bras and M. Sharma, *Nat. Genet.*, 2014, **46**, 989.
4 M. Xilouri, O. R. Brekk and L. Stefanis, *Mol. Neurobiol.*, 2013, **47**, 537–551.
5 S. Kaushik and A. M. Cuervo, *Nat. Med.*, 2015, **21**, 1406.
6 W. Poewe, K. Seppi, C. M. Tanner, G. M. Halliday, P. Brundin, J. Volkmann, A.-E. Schrag and A. E. Lang, *Nat. Rev. Dis. Primers*, 2017, **3**, 17013.
7 W. Le, J. Dong, S. Li and A. D. Korczyn, *Neurosci. Bull.*, 2017, **33**, 535–542.
8 L. Parnetti, A. Castrioto, D. Chiasserini, E. Persichetti, N. Tambasco, O. El-Agnaf and P. Calabresi, *Nat. Rev. Neurol.*, 2013, **9**, 131.
9 Z. Hong, M. Shi, K. A. Chung, J. F. Quinn, E. R. Peskind, D. Galasko, J. Jankovic, C. P. Zabetian, J. B. Leverenz and G. Baird, *Brain*, 2010, **133**, 713–726.
10 Y. Wu, W. Le and J. Jankovic, *Arch. Neurol.*, 2011, **68**, 22–30.
11 C. Marras and A. Lang, *J. Neurol., Neurosurg. Psychiatry*, 2013, **84**(4), 409–415.
12 A. Atik, T. Stewart and J. Zhang, *Brain Pathol.*, 2016, **26**, 410–418.
13 L. Stefanis, *Cold Spring Harbor Perspect. Med.*, 2012, **2**, a009399.
14 J. Bergström and M. Ingelsson, *Immunotherapy and Biomarkers in Neurodegenerative Disorders*, 2016, pp. 215–234.
15 L. Gao, H. Tang, K. Nie, L. Wang, J. Zhao, R. Gan, J. Huang, R. Zhu, S. Feng and Z. Duan, *Int. J. Neurosci.*, 2015, **125**, 645–654.
16 A. Shalash, M. Salama, M. Makar, T. Roushdy, H. H. Elrassas, W. Mohamed, M. El-Balkimy and M. Abou Donia, *Front. Neurol.*, 2017, **8**, 720.
17 L. Parnetti, D. Chiasserini, E. Persichetti, P. Eusebi, S. Varghese, M. M. Qureshi, A. Dardis, M. Deganuto, C. Carlo and A. Castrioto, *Mov. Disord.*, 2014, **29**, 1019–1027.
18 M. Delenclos, D. R. Jones, P. J. McLean and R. J. Uitti, *Parkinsonism Relat. Disord.*, 2016, **22**, S106–S110.
19 K. Henriksen, S. E. O'Bryant, H. Hampel, J. Q. Trojanowski, T. J. Montine, A. Jeromin, K. Blennow, A. Lönneborg, T. Wyss-Coray and H. Soares, *Alzheimer's Dementia*, 2014, **10**, 115–131.
20 M. Politis, *Nat. Rev. Neurol.*, 2014, **10**, 708.
21 K. M. Bell and S. E. Kornguth, *Handbook of Biosensors and Biochips*, 2007.
22 H. V. Ganesh, A. M. Chow and K. Kerman, *TrAC, Trends Anal. Chem.*, 2016, **79**, 363–370.
23 B. Shui, D. Tao, A. Florea, J. Cheng, Q. Zhao, Y. Gu, W. Li, N. Jaffrezic-Renault, Y. Mei and Z. Guo, *Biochimie*, 2018, 13–24.
24 S. Bouden, A. Dahi, F. Hauquier, H. Randriamahazaka and J. Ghilane, *Sci. Rep.*, 2016, **6**, 36708.
25 K. Grochowska, K. Siuzdak and G. Śliwiński, *Eur. J. Inorg. Chem.*, 2015, **2015**, 1275–1281.
26 B. Demirbakan and M. K. Sezgintürk, *Talanta*, 2017, **169**, 163–169.
27 Y. Ma, J. Di, X. Yan, M. Zhao, Z. Lu and Y. Tu, *Biosens. Bioelectron.*, 2009, **24**, 1480–1483.
28 D. P. Santos, M. V. B. Zanoni, M. F. Bergamini, A.-M. Chiorcea-Paquim, V. C. Diculescu and A.-M. O. Brett, *Electrochim. Acta*, 2008, **53**, 3991–4000.
29 M. N. S. Karaboğa and M. K. Sezgintürk, *Talanta*, 2018, **186**, 162–168.
30 L. Wang, W. Mao, D. Ni, J. Di, Y. Wu and Y. Tu, *Electrochem. Commun.*, 2008, **10**, 673–676.
31 T. Hezard, K. Fajerwerg, D. Evrard, V. Collière, P. Behra and P. Gros, *J. Electroanal. Chem.*, 2012, **664**, 46–52.
32 J. S. Daniels and N. Pourmand, *Electroanalysis*, 2007, **19**, 1239–1257.
33 J. J. Harris and M. L. Bruening, *Langmuir*, 2000, **16**, 2006–2013.
34 B. A. Boukamp, *J. Electrochem. Soc.*, 1995, **142**, 1885–1894.
35 P. Agarwal, M. E. Orazem and L. H. Garcia-Rubio, *J. Electrochem. Soc.*, 1992, **139**, 1917–1927.
36 J. Goode, J. Rushworth and P. Millner, *Langmuir*, 2014, **31**, 6267–6276.
37 A. Chen and B. Shah, *Anal. Methods*, 2013, **5**, 2158–2173.
38 A. F. Hühmer, R. G. Biringer, H. Amato, A. N. Fonteh and M. G. Harrington, *Dis. Markers*, 2006, **22**, 3–26.

39 E. Kapaki, G. P. Paraskevas, E. Emmanouilidou and K. Vekrellis, *PLoS One*, 2013, **8**, e81654.
40 Y. An, L. Tang, X. Jiang, H. Chen, M. Yang, L. Jin, S. Zhang, C. Wang and W. Zhang, *Chem. – Eur. J.*, 2010, **16**, 14439–14446.
41 Y. An, X. Jiang, W. Bi, H. Chen, L. Jin, S. Zhang, C. Wang and W. Zhang, *Biosens. Bioelectron.*, 2012, **32**, 224–230.
42 K. Sun, N. Xia, L. Zhao, K. Liu, W. Hou and L. Liu, *Sens. Actuators, B*, 2017, **245**, 87–94.